Investigation of structural morphology and electrical properties of graphene-C_{60} hybrids

Srishti ChughChandan BiswasLuis EchegoyenAnupama B. Kaul

Citation: Journal of Vacuum Science & Technology B, Nanotechnology and Microelectronics: Materials, Processing, Measurement, and Phenomena **35**, 03D111 (2017); doi: 10.1116/1.4982881

View online: http://dx.doi.org/10.1116/1.4982881

View Table of Contents: http://avs.scitation.org/toc/jvb/35/3

Published by the American Vacuum Society

Investigation of structural morphology and electrical properties of graphene-C_{60} hybrids

Srishti Chugh
Department of Metallurgical, Materials and Biomedical Engineering, University of Texas at El Paso, El Paso, Texas 79968

Chandan Biswas
Department of Electrical and Computer Engineering, University of Texas at El Paso, El Paso, Texas 79968

Luis Echegoyen
Department of Chemistry, University of Texas at El Paso, El Paso, Texas 79968

Anupama B. Kaul[a)]
Department of Electrical and Computer Engineering, University of Texas at El Paso, El Paso, Texas 79968

(Received 15 January 2017; accepted 20 April 2017; published 2 May 2017)

In this work, the authors report on the electrophoretic deposition of C_{60} on graphene. The graphene films were characterized using Raman spectroscopy and scanning electron microscopy, and electrical contacts were made with the graphene nanomembranes using a viscoelastic stamping method. Different concentration solutions of C_{60} were prepared and deposited on graphene substrates using the electrophoretic deposition technique. Electronic characterization of the structures was conducted before and after the attachment of C_{60}. Optical absorption of different concentrations of C_{60} was measured. A comparative study was carried out to analyze the resistivity and conductivity as a result of the interaction with a Si/SiO_2 substrate. Our results suggest that graphene based C_{60} structures are attractive as flexible transparent electrodes and are excellent electron accepting/charge transport materials for the construction of efficient photovoltaic devices. © *2017 American Vacuum Society*. [http://dx.doi.org/10.1116/1.4982881]

I. INTRODUCTION

Graphene is a two-dimensional sp^2 hybridized material composed of carbon atoms arranged in a hexagonal atomic structure, which has attracted a lot of attention because of its unique electrical properties such as very high carrier mobility,[1–5] the Quantum hall effect at room temperature,[3–6] and ambipolar electric field effects along with ballistic conduction of charge carriers.[7] These unique features hold great promise for potential applications in many technological fields, such as lithium batteries.[3] Other allotropes of carbon such as fullerenes[8] (C_{60} and others) and one-dimensional carbon nanotubes[9] (CNTs) have attracted strong interest in many areas of science and technology. Nanocarbons, both in pure forms and in hybrid structures, give rise to unique electronic and structural properties and have the potential to be used as building blocks in molecular electronic devices.[10–13] Higher fullerenes and C_{60} show remarkable chemical reactivity. Various hybrid materials created by organic functionalization of fullerenes have attracted intense attention, driven by the possibility of combining some of the outstanding properties of the fullerenes with those of other interesting materials, such as photoactive and/or electroactive units, including small organic molecules, polymers, and CNTs. These structures are promising organic materials in many applications such as field effect transistors,[14] organic solar cells,[15] and organic light emitting diodes.[16] Given that many applications of C_{60} have been assessed as molecular layers on supporting substrates, much of this effort has thus far been focused on gaining precise information about the behavior of fullerenes on various surfaces. For example, Shen *et al.*[17] reported that C_{60}-CNT hybrid materials can be used to produce excellent electrodes for photovoltaic applications and that CNT field effect transistors decorated with C_{60} composites show potential as highly sensitive photosensors. Nasibulin *et al.*[18] prepared a CNT-C_{60} hybrid material which showed a high cold electron field emission efficiency, potentially interesting for many optoelectronic applications. The deposition of C_{60} on single layer graphene was done using different methods such as drop-casting or reduction of single layer graphene to graphene oxide followed by electrochemistry and thermal evaporation of C_{60} on graphene. These methods facilitated the deposition of C_{60} on the graphene and reduced the degree of the resulting agglomeration, but the resulting films were not uniform enough and C_{60} was deposited everywhere, thus making it difficult to make electrical measurements.[19–21] Herein, we report a new technique to synthesize graphene-C_{60} hybrid materials via electrophoretic deposition of C_{60} from a colloidal suspension of C_{60} in toluene-acetonitrile so that C_{60} clusters are formed and deposited uniformly on the exfoliated graphene for electrical measurements.

II. EXPERIMENT

Figure 1 presents the schematic of the electrophoretic deposition system for C_{60} on a graphene nanomembrane. The graphene nanomembrane was mechanically exfoliated from HOPG and was placed on a residue-free scotch-tape. A viscoelastic stamping method was used[22] to transfer the

[a)]Electronic mail: akaul@utep.edu

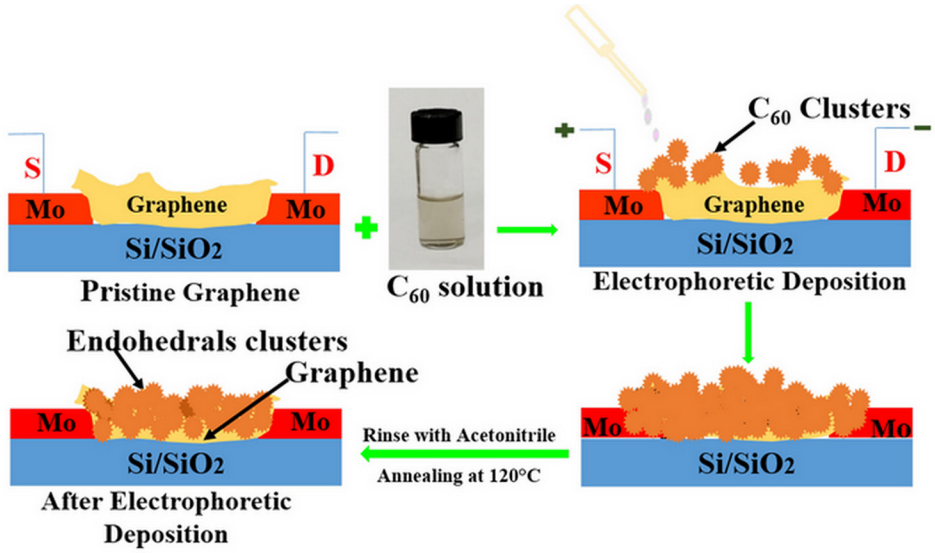

FIG. 1. (Color online) Schematic representation of the electrophoretic deposition process for depositing C_{60} on top of graphene.

graphene nanomembrane to the desired electrode. Figure 2 shows the source–drain current measurements as a function of electrophoretic deposition time. Since C_{60} films cannot be deposited directly on the graphene surface, therefore, the clusters were prepared in mixed solvents. Different concentration solutions of C_{60} in toluene (5, 19, 35, and 45 μM) were mixed with acetonitrile:toluene (3:1 v/v). In the presence of a polar solvent such as acetonitrile, the clusters can be charged, thus facilitating their deposition on the electrode surface.[23] A drop of the suspension was injected, and a step potential was applied (from 0.05 to 0.3 V with 0.05 V step) between source/drain of Mo contacts of the device on the electrode for the electrophoretic deposition. The current increased gradually as the step-potential was increased with time. At certain intervals of time, the current saturates and starts to decrease because of Joule heating in the channel as the resistance increases.

These instantaneous current peaks in the device could be caused by charge transfer from the attached C_{60} clusters to

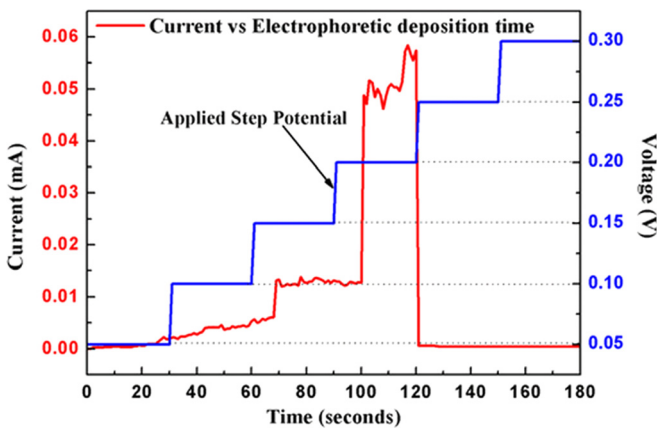

FIG. 2. (Color online) Current-source measurement of the device in toluene-acetonitrile solution. Step potential (from 0.05 to 0.3 V with a step of 0.05 V in the interval of 30 s) applied to the device immersed in 19 μM of C_{60} in toluene in 3:1 (v/v) acetonitrile:toluene.

the graphene nanomembrane. The strong van der Waals interactions lead to C_{60} attachment to the graphene surface.[24] Within 120 s, all the C_{60} clusters were deposited as a brown film on the graphene nanomembrane, and no further accumulation of C_{60} was observed after 120 s. The reason for this color change is the relatively narrow energy width of the band responsible for green light absorption by individual C_{60} molecules. Individual molecules transmit some blue and red light, resulting in a purple color or a nearly transparent color depending upon the concentration of the solvent. Upon drying, intermolecular interactions result in the overlap and broadening of the energy bands, thereby eliminating the blue light transmittance and causing the purple to brown color change.[25] The clusters varied in size depending on the different concentrations used.

Finally, the graphene-C_{60} hybrids obtained were rinsed with acetonitrile and annealed at 120 °C for 2 min to remove any further toluene residue. The clusters did not wash away after rinsing the graphene-C_{60} hybrids with acetonitrile solution and remained attached to the graphene nanomembranes due to intermolecular interactions between C_{60} and graphene, and thus the clusters were robust.[37] Electrical measurements of the graphene-C_{60} hybrids were carried out and investigated using Raman spectroscopy and optical absorption for different C_{60} concentrations.

III. RESULTS AND DISCUSSION

The thickness of the hybrids obtained was measured using a Bruker DektakXT Stylus Profiler. As the concentration of C_{60} is increased, the thickness of the hybrids increased. The thickness of the graphene nanomembrane was measured to be 62.05 nm, while the thickness of the hybrids (graphene-C_{60}) formed using 5, 19, 35, and 45 μM of fullerenes were determined to be 70, 80.13, 101.5, and 150.56 nm, respectively. Figure 3 shows the absorption of different concentrations of C_{60} (5, 19, 35, and 45 μM) in toluene solution. C_{60} exhibits a structureless broad absorption in the 400–700 nm

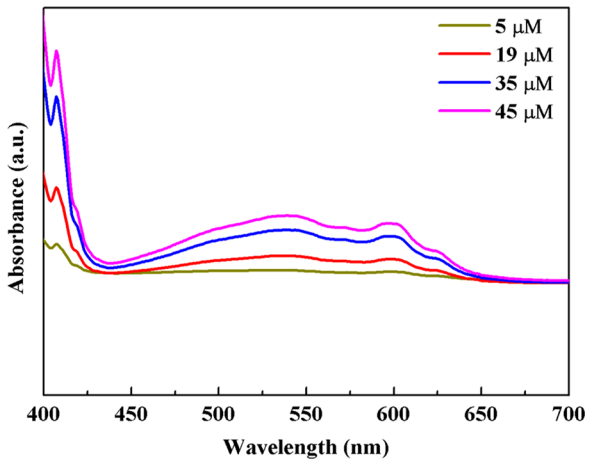

FIG. 3. (Color online) Absorbance of different concentrations of C_{60} in toluene as a function of wavelength.

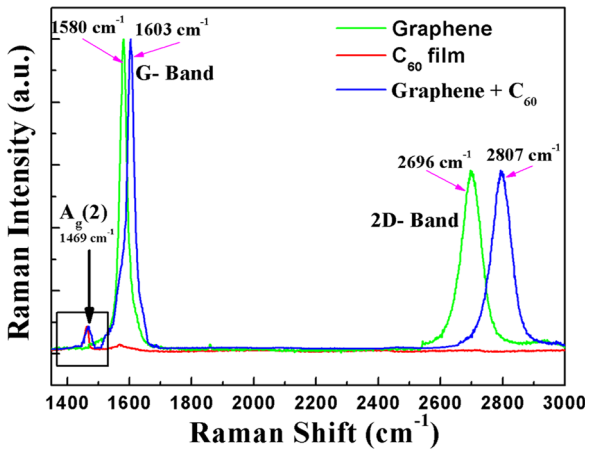

FIG. 5. (Color online) Raman spectra showing shifts toward higher frequencies for the G and 2D bands of graphene after electrophoretic deposition of C_{60}. The Raman spectrum of the C_{60} film is dominated by the pentagonal pinch mode A_g (2) at 1469 cm^{-1}. The peaks are shifted toward higher frequencies as C_{60} clusters in the deposited film act as electron acceptors, yielding increased hole doping in the graphene layer.

region. The principal band in the 410 nm range is mainly due to orbitally allowed singlet-singlet transitions. A broad weak continuum between 430 and 640 nm, whose maximum is at about 540 nm, appears to be due to vibronic bands based on electronic transitions from the lowest unoccupied molecular orbital to the three-fold degenerate $1T_{1u}$ state and to the other degenerate states. The absorbance of the solution was increased with an increase in the concentration of C_{60}. Also, the color of the C_{60} solution changes depending on the solvent and the concentration of C_{60}. The changes in color may arise from the difference in the size of C_{60} clusters, structure, and/or interactions between the colloidal C_{60} particles and the solvent molecules.[26–30] The SEM measurements were carried out to determine the aggregation and the shape of the clusters after deposition on the graphene nanomembranes. Figure 4 shows the SEM of (a) graphene and (b) graphene-C_{60} hybrids after electrophoretic deposition. The graphene nanomembranes were mechanically exfoliated several times using the scotch tape method due to which the graphene film appeared to be discontinuous when seen through the SEM. The C_{60} clusters aggregated on top of the graphene nanomembranes.

Raman spectroscopy of the graphene nanomembrane and graphene-C_{60} hybrids was also conducted at room temperature as shown in Fig. 5. Raman spectroscopy is a useful technique for characterizing sp^2 and sp^3 hybridized carbon atoms, including those in graphite, fullerenes, carbon nanotubes, and graphene.[31–35] The prominent G-mode and 2D-mode peaks of single layer graphene[36] appear at around 1580 and 2700 cm^{-1}. The mechanically exfoliated graphene nanomembranes show an intense tangential mode (G band) at 1580 cm^{-1} and a 2D band at 2696 cm^{-1}. The I_{2D}/I_G ratio was 0.59, indicating a few layer graphene (FLG).

A negligible D-band was obvious in the sample due to the highly crystalline nature. The graphene-C_{60} hybrid shows three peaks at 1469, 1603, and 2807 cm^{-1}. The graphene G and 2D band peaks are shifted to higher frequencies at 1603

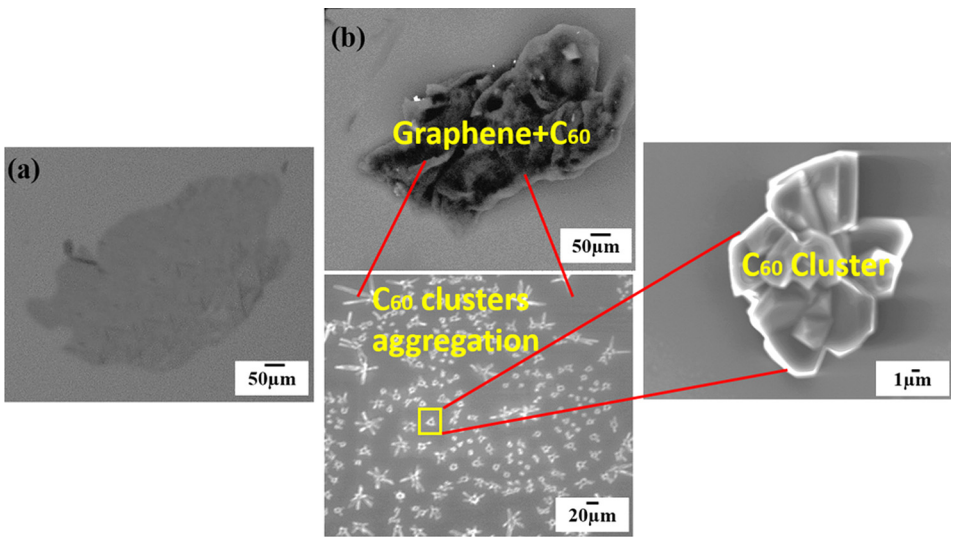

FIG. 4. (Color online) Top view SEM images of (a) graphene and (b) graphene-C_{60} hybrid.

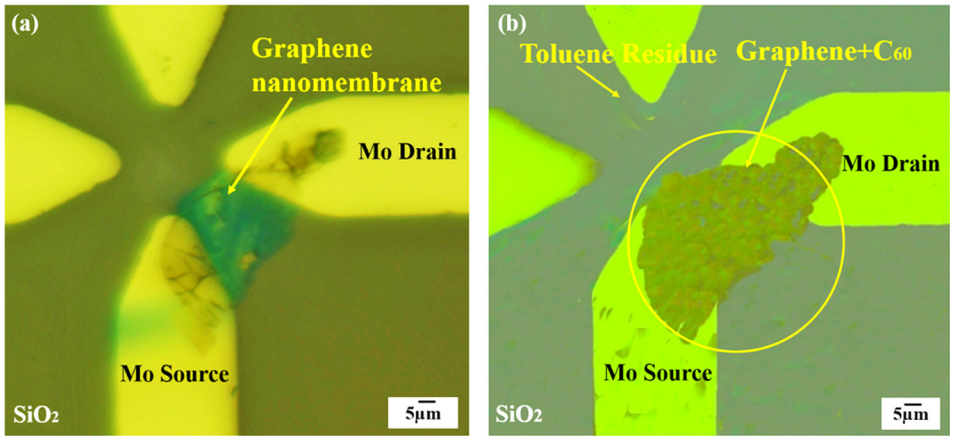

FIG. 6. (Color online) Optical micrographs of (a) FLG nanomembranes transferred on top of 100 nm Mo electrodes using a viscoelastic stamping method and (b) C_{60} deposited on the graphene nanomembranes using electrophoretic deposition.

and 2807 cm^{-1} as C_{60} clusters deposited act as electron acceptors, yielding increased hole doping in the graphene layer.[26] The peak at 1469 cm^{-1} can be assigned to the $A_g(2)$ mode of the C_{60} cage. This is the strongest Raman line of the C_{60} film with the "pentagonal pinch mode." The pentagonal pinch mode involves 100% tangential displacement of the C-atoms on the ball so as to shrink the pentagons and expand the hexagons.[25] This relatively high shift suggests a strong interaction between the C_{60} cages and the graphene sheet.[37]

In order to investigate the electronic transport properties of the graphene-C_{60} hybrids prepared with different concentrations of C_{60}, electrical contacts were made. Figure 6(a) shows the optical micrograph of FLG nanomembranes transferred on top of 100 nm molybdenum (Mo) electrodes using a viscoelastic stamping method,[22] and Fig. 6(b) shows the optical micrograph of C_{60} deposited on the same graphene nanomembranes using electrophoretic deposition. IV measurements were performed to compare the electrical behavior of the hybrids with that of graphene. Figure 7(a) shows the variation of current with voltage for the graphene nanomembrane and for the graphene-C_{60} hybrids prepared with different concentrations of C_{60}, measured at a 2 μm probe separation distance. Under direct contact of C_{60} and FLG, electrons diffuse to C_{60} creating holes in the graphene due to which the current values change for the graphene-C_{60} hybrids of different concentrations. The graphene is initially p-type, and the increase in the hole population causes the conductivity of the hybrids to also increase. During the electrophoretic deposition process, aggregation of C_{60} molecules takes place in mixed solvents. The C_{60} molecules coalesce and aggregate but do not form a continuous film, and thus, the conductance of C_{60} deposited electrophoretically was negligible.[40] On the other hand, the graphene-C_{60} hybrid devices showed reproducible conductive behavior originating from the electron-accepting nature of the C_{60} molecules.[26]

It should be noted that there exists a high affinity between the graphite lattice structure and C_{60} derivatives.[38,39] The IV plot always remains linear, but the slope increased with increasing concentration of C_{60}. Figure 7(b) shows the variation of resistance of the hybrids with different concentrations of C_{60} in toluene in 3:1 (v/v) acetonitrile:toluene. The resistance for the graphene nanomembranes was 226 Ω, and the resistance obtained for graphene + 5 μM of C_{60}, graphene + 19 μM of C_{60}, graphene + 35 μM of C_{60}, and graphene + 45 μM of C_{60} in toluene in 3:1 (v/v) acetonitrile:toluene were 2942,117, 748, and 392 Ω. The resistance values show that there was charge transfer from the graphene to C_{60}. This may be due to the hybrid formed. The variation of resistance of the hybrids with the different concentrations of C_{60}

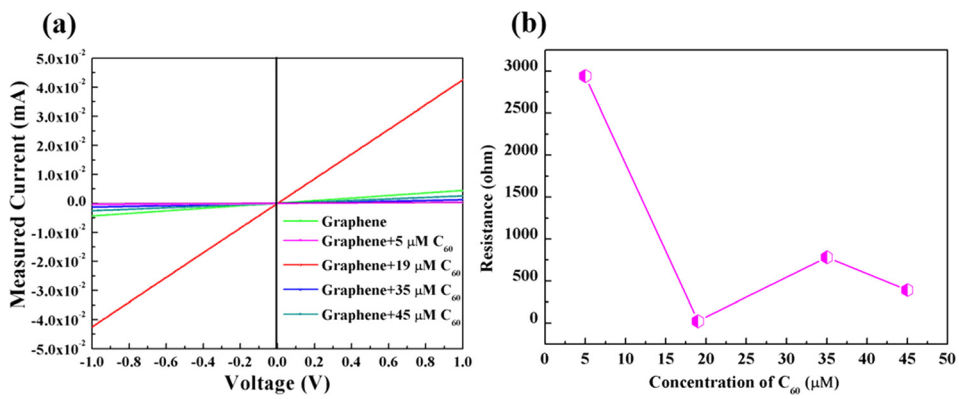

FIG. 7. (Color online) (a) IV characteristics of graphene and graphene-C_{60} hybrids; (b) Variation of resistance of the graphene-C_{60} hybrids with different concentrations of C_{60} in toluene in 3:1 (v/v) acetonitrile:toluene.

reflects that graphene functions as a charge transporting layer to enhance conduction. These results suggest that there was aggregation of C_{60} clusters on top of the graphene nanomembranes due to the adsorption of fullerenes on pristine graphene, which is governed by van der Waals interactions. The fullerenes physisorbed on graphene layers are stable and have charge transfer between the components,[41,42] which is mainly associated with the strong three-dimensional hydrophobic interactions between C_{60} and graphene.[40]

IV. CONCLUSION

In conclusion, we have synthesized a graphene-C_{60} hybrid material using an electrophoretic deposition technique and analyzed using Raman spectroscopy. The peak shifts in Raman spectroscopy to higher frequencies show the intermolecular interactions of the graphene and C_{60}. The graphene-C_{60} hybrids show that there was a charge transfer from the graphene to C_{60}. The increase in the hole population causes the conductivity of the hybrids to also increase, which shows that the material could exhibit some distinctive electronic/optoelectronic properties. This hybrid material may find applications in solar cells as an acceptor material. Further work on applications of this hybrid material is currently under way.

ACKNOWLEDGMENTS

A.B.K. acknowledges the University of Texas System Faculty Science and Technology Acquisition and Retention (STARS) award (EC284802) for the acquisition of equipment in the establishment of the Nanomaterials and Devices Lab at the University of Texas, El Paso (UTEP). The authors also thank the Army Research Office (ARO W911NF-15-1-0425) that enabled us to pursue this work. L.E. thanks the NSF for generous support of this work under grant (CHE-1408865) and the NSF-PREM program (DMR-1205302). The Robert A. Welch Foundation is also gratefully acknowledged for an endowed chair to L.E. (Grant No. AH-0033).

[1]A. K. Geim and K. S. Novoselov, Nat. Mater. **6**, 183 (2007).
[2]K. S. Novoselov, A. K. Geim, S. V. Morozov, D. Jiang, Y. Zhang, S. V. Dubonos, I. Grigorieva, and A. A. Firsov, Science **306**, 666 (2004).
[3]K. S. Novoselov and A. K. Geim, Nature **438**, 197 (2005).
[4]C. N. R. Rao, A. K. Sood, K. S. Subrahmanyam, and A. Govindraj, Angew. Chem. Int. Ed. **48**, 7752 (2009).
[5]J. H. Chen, C. Jang, S. Xiao, M. Ishigami, and M. S. Fuhrer, Nat. Nanotechnol. **3**, 206 (2008).
[6]M. Y. Han, B. Oezyilmaz, Y. Zhang, and P. Kim, Phys. Rev. Lett. **98**, 206805 (2007).
[7]E. Yoo, J. Kim, E. Hosono, H. S. Zhou, T. Kudo, and I. Honma, Nano Lett. **8**, 2277 (2008).
[8]W. Kratschmer, L. D. Lamb, K. Fostiropoulos, and D. R. Huffman, Nature **347**, 354 (1990).
[9]X. Wang, Q. Li, J. Xie, Z. Jin, J. Wang, Y. Li, K. Jiang, and S. Fan, Nano Lett. **9**, 3137 (2009).
[10]F. Wudl, J. Mater. Chem. **12**, 1959 (2002).
[11]A. H. C. Neto, F. Guinea, N. M. R. Peres, K. S. Novoselov, and A. K. Geim, Rev. Mod. Phys. **81**, 109 (2009).
[12]M. J. Allen, V. C. Tun, and R. B. Kaner, Chem. Rev. **110**, 132 (2010).
[13]M. Batzill, Surf. Sci. Rep. **67**, 83 (2012).
[14]M. Funahashi, F. P. Zhang, and N. Tamaoki, Adv. Mater. **19**, 353 (2007).
[15]N. Matín, L. Sánchez, M. A. Herranz, B. Illescas, and D. M. Guldi, Acc. Chem. Res. **40**, 1015 (2007).
[16]K. Hutchison, J. Gao, G. Schick, Y. Rubin, and F. Wudl, J. Am. Chem. Soc. **121**, 5611 (1999).
[17]Y. Shen *et al.*, Chem. Sci. **2**, 2243 (2011).
[18]A. G. Nasibulin, P. V. Pikhitsa, H. Jiang, D. P. Brown, A. V. Krasheninnikov, and A. S. Anisimov, Nat. Nanotechnol. **22**, 156 (2007).
[19]V. Georgakilas, A. B. Bourlinos, E. Ntararas, A. Ibraliu, D. Gournis, K. Dimos, A. Kouloumpis, and R. Zboril, Carbon **110**, 51 (2016).
[20]M. Barrejón *et al.*, Chem. Commun. **50**, 9053 (2014).
[21]J. Yang, M. Heo, H. J. Lee, S. M. Park, J. Y. Kim, and H. S. Shin, ACS Nano **5**, 8365 (2011).
[22]A. C. Gomez, M. Buscema, R. Molenaar, V. Singh, L. Janssen, H. S. J. Zant, and G. A. Steele, 2D Mater. **1**, 011002 (2014).
[23]P. V. Kamat, S. Barazzouk, K. G. Thomas, and S. Hotchandani, J. Phys. Chem. B **104**, 4014 (2000).
[24]K. Kim, T. H. Lee, E. J. G. Santos, P. S. Jo, A. Salleo, Y. Nishi, and Z. Bao, ACS Nano **9**, 5922 (2015).
[25]M. Dresselhaus, G. Dresselhaus, and P. C. Eklund, *Science of Fullerenes and Carbon Nanotubes* (Academic, 1996), p. 437.
[26]G. Jnawali, Y. Rao, J. H. Beck, N. Petrone, I. Kymissis, J. Hone, and T. F. Heinz, ACS Nano **9**, 7175 (2015).
[27]S. Leach, M. Vervloet, A. Desprès, E. Bréheret, J. P. Hare, T. J. Dennis, H. W. Kroto, R. Taylor, and D. R. M. Walton, Chem. Phys. **160**, 451 (1992).
[28]M. A. Greaney and S. M. Gorun, J. Phys. Chem. **95**, 7142 (1991).
[29]E. Menendez-Proupin, A. Delgado, A. L. M. Alejo, and J. M. García de la Vega, Chem. Phys. Lett. **593**, 72 (2014).
[30]S. H. Gallagher, R. S. Armstrong, P. A. Lay, and C. A. Reed, J. Phys. Chem. **99**, 5817 (1995).
[31]S. Gayathri, P. Jayabal, M. Kottaisamy, and V. Ramakrishnan, AIP Adv. **4**, 027116 (2014).
[32]L. Bokobza, J. L. Bruneel, and M. Couzi, Vib. Spectrosc. **74**, 57 (2014).
[33]A. C. Ferrari, Solid State Commun. **143**, 47 (2007).
[34]A. C. Ferrari Ferrari *et al.*, Phys. Rev. Lett. **97**,187401 (2006).
[35]L. M. Malard, M. A. Pimenta, G. Dresselhaus, and M. S. Dresselhaus, Phys. Rep. **473**, 51 (2009).
[36]R. P. Vidano, D. B. Fischbach, L. J. Willis, and T. M. Loehr, Solid State Commun. **39**, 341 (1981).
[37]J. L. Delgado, P. de la Cruz, F. Langa, A. Urbina, J. Casado, and J. T. Lopez Navarrete, Chem. Commun. **104**, 1734 (2004).
[38]T. Tajima, W. Sakata, T. Wada, A. Tsutsui, S. Nishimoto, M. Miyak, and Y. Takaguchi, Adv. Mater. **23**, 5750 (2011).
[39]T. Umeyama, N. Tezuka, M. Fujita, S. Hayashi, N. Kadota, Y. Matano, and H. Imahori, Chem. Eur. J. **14**, 4875 (2008).
[40]Y. M. Wang, P. V. Kamat, and L. K. Patterson, J. Phys. Chem. **97**, 8793 (1993).
[41]M. Švec, P. Merino, Y. Dappe, C. González, E. Abad, P. Jelínek, and J. Martín-Gago, Phys. Rev. B **86**, 121407 (2012).
[42]S. Laref, A. Asaduzzaman, W. Beck, P. A. Deymier, K. Runge, L. Adamowicz, and K. Muralidharan, Chem. Phys. Lett. **582**, 115 (2013).